Structures and Dynamic Formation Processes of Porphyrin Adlayers on Iodine-Modified Au(111) in Solution: In Situ STM Study

ARTICLE *in* LANGMUIR · MARCH 1997

Impact Factor: 4.46 · DOI: 10.1021/la9620216

4 AUTHORS, INCLUDING:

Masashi Kunitake
Kumamoto University
150 PUBLICATIONS **2,055** CITATIONS

SEE PROFILE

Kingo Itaya
Tohoku University
245 PUBLICATIONS **8,273** CITATIONS

SEE PROFILE

Structures and Dynamic Formation Processes of Porphyrin Adlayers on Iodine-Modified Au(111) in Solution: In Situ STM Study

Masashi Kunitake, Uichi Akiba, Nikola Batina,† and Kingo Itaya*

Itaya Electrochemiscopy Project, ERATO, JRDC, 2-1-1 Yagiyama-Minami, Sendai 982, Japan

Received November 19, 1996⊗

The structures and dynamic formation processes of adlayers of 5,10,15,20-tetrakis(*N*-methylpyridinium-4-yl)-21*H*,23*H*-porphine (TMPyP) on both bare Au(111) and iodine-modified Au(111) in perchloric acid have been investigated in detail by using in situ scanning tunneling microscopy (STM). Highly-ordered TMPyP arrays formed on iodine-modified Au(111), whereas disordered adlayers were consistently found on bare Au(111) surface. High-resolution STM images revealed the characteristic internal shape and orientation of each TMPyP molecule in ordered adlayers. Time-dependent in situ STM allowed direct observation of the dynamics of the self-ordering processes. Before the most stable adlayer was established in a relatively small domain, several structural changes were found to occur, including the formation of a one-dimensional ordered chain at an early stage and several phase transitions in the ordered adlayers. Once the most stable adlayer was formed as a nucleus in a domain, two-dimensional growth of the domain extended over the entire area of the terraces with the final packing arrangement.

Introduction

Scanning tunneling microscopy (STM) has made it possible to directly determine orientations, packing arrangements, and even internal structures of organic molecules adsorbed both on surfaces and at interfaces.[1,2] For example, individual molecules and distinguishable molecular shapes of benzene on Pt(111),[3] coadsorbed benzene and CO on Rh(111),[4] naphthalene on Pt(111),[5] and copper phthalocyanine on Cu(100)[6] have successfully been resolved with STM under ultrahigh-vacuum (UHV) conditions. These results have stimulated a large number of STM studies of ordered molecular adlayers in UHV and air as well as at solid−liquid interfaces because of their wide range of applications in catalysis,[7] electrocatalysis,[8] biology[9] and future molecular devices at the nanometer scale.[10]

A variety of experimental procedures have been reported for the preparation of ordered molecular adlayers on well-defined substrates including single crystals of metals and layered materials such as highly ordered pyrolytic graphite (HOPG) and MoS_2.[1,2,9] Alkanethiols have been intensively investigated on Au surfaces,[11] because the −SH group is known to be chemically attached to the Au surface through the formation of a covalent bond between S and Au atoms, producing densely-packed adlayers. Ag(111) has also been used for the investigation of the adsorption of alkanethiols.[12] On the other hand, it is well-known that simple physical adsorption can also provide ordered adlayers of molecules such as liquid crystals[13] and *n*-alkanes[14] on inert substrates such as HOPG and MoS_2. The Langmuir−Blodgett technique has long been applied to many amphiphilic molecules, in which ordered monolayers formed at the water−air interface can be transferred onto various substrates.[15]

From the electrochemical point of view, the adsorption of organic molecules at electrode−electrolyte interfaces can be considered as one of the most promising approaches not only for the preparation of ordered adlayers but also for elucidating the role of properties of adsorbed molecules and the nature of electrode−electrolyte interfaces.[16−18] In spite of a large number of reports describing the observation by STM and related techniques such as atomic force microscopy (AFM) of adsorbed organic molecules in UHV, air, and organic liquids, few in situ STM studies have been carried out for organic molecules adsorbed at electrode−electrolyte interfaces under electrochemical conditions.[19] Recently, however, reports have shown high-

* To whom correspondence should be addressed at the Department of Applied Chemistry, Faculty of Engineering, Tohoku University, Sendai 980, Japan

† Current address: Departamento de Quimica, Universidad Automa Metrolitana-Iztapalapa, Apartado Postal 55-534, 09340 Mexico.

⊗ Abstract published in *Advance ACS Abstracts,* February 1, 1997.

(1) Chiang, S. In *Scanning Tunneling Microscopy I*; Wiesendanger, R., Guntherodt, H. J., Eds.; Springer-Verlag: Berlin, 1991; p 181.

(2) Rabe, J. P. *Ultramicroscopy* **1992**, *42*−*44*, 41, and references cited therein.

(3) Weiss, P. S.; Eigler, D. M. *Phys. Rev. Lett.* **1993**, *71*, 3139.

(4) Ohtani, H.; Wilson, R. J.; Chiang, S.; Mate, C. M. *Phys. Rev. Lett.* **1988**, *60*, 2398.

(5) Hallmark, V. M.; Chiang, S.; Brown, J. K.; Woll, Ch. *Phys. Rev. Lett.* **1991**, *66*, 48.

(6) (a) Lippel, P. H.; Wilson, R. J.; Miller, M. D.; Woll, C.; Chiang, S. *Phys. Rev. Lett.* **1989**, *62*, 171. (b) Fritz, T.; Hara, M.; Knoll, W.; Sasabe, H. *Mol. Cryst. Liq. Cryst.* **1994**, *253*, 269.

(7) Somorjai, A. T. In *Introduction to Surface Chemistry and Catalysis I*; John Wiley & Sons Inc.: New York, 1994.

(8) Bard, A. J.; Abruna, H. D.; Chidsey, C. E.; Faulkner, L. R.; Feldberg, S. W.; Itaya, K.; Majda, M.; Merloy, O.; Murray, R. W.; Porter, M. D.; Soriaga, M. P.; White, H. S. *J. Phys. Chem.* **1993**, *97*, 7147.

(9) Guckenberger, R.; Hartmann,T.; Wiegrabe, W.; Baumeister, W. In *Scanning Tunneling Microscopy II*; Wiesendanger, R., Guntherodt, H. J., Eds.; Springer-Verlag: New York, 1991; Vol. 20; Chapter 3.

(10) Richardson, T.; Hara, M.; Sasabe, H. In *An Introduction to Molecular Electronics*; Petty, M. C., Bryce, M. R., Bloor, D., Eds.; Edward Arnold: London, 1995, p 220.

(11) (a) Alves, C. A.; Smith, E. L.: Porter, M. D. *J. Am. Chem. Soc.* **1992**, *114*, 1222. (b) Stranick, S. J.; Parikh, A. N.; Tao, Y. T.; Allara, D. L.; Weiss P. S. *J. Phys. Chem.* **1994**, *98*, 7636. (c) Poirier, G. E.; Tarlov, M. J. *Langmuir* **1994**, *10*, 2853. (d) Sprik, M.; Dalamarche, E.; Michel, B.; Rothlisberger, U. ; Klein, M. L.; Wolf, H.; Ringsdorf, H. *Langmuir* **1994**, *10*, 4116. (e) Caldwell, W. B.; Campbell, D. J.; Chen, K.; Herr, B. R.; Mirkin, C. A.; Malik, A.; Durbin, M. K.; Dutta, P.; Huang, K. G. *J. Am. Chem. Soc.* **1995**, *117*, 6071. (f) Poirier, G. E.; Pylant, E. D.; *Science* **1996**, *272*, 1145.

(12) Heinz, R.; Rabe, J. P. *Langmuir* **1995**, *11*, 506.

(13) (a) Smith, D. P. E.; Horber, J. K. H.; Binnig, G.; Nejoh, H. *Nature* **1990**, *344*, 641. (b) Walba, D. M.; Stevens, F.; Parks, D. C.; Clark, N. A.; Wand, M. D. *Science* **1995**, *267*, 1144.

(14) (a) Stabel, A.; Heinz, R.; De Schryver, F. C.; Rabe, J. P. *J. Phys. Chem.* **1995**, *99*, 505. (b) Hibino, M.; Sumi, A.; Hatta, I. *Jpn. J. Appl. Phys.* **1995**, *34*, 610.

(15) For example: Kuhn, H. *Thin Solid Films* **1989**, *178*, 1.

(16) Lipkowski, J.; Ross, P. N., Eds. *Adsorption of Molecules at Metal Electrodes*; VCH Publishers: New York, 1992.

(17) Hubbard, A. T. *Chem. Rev.* **1988**, *88*, 633.

(18) Soriaga, M. P. *Progr. Surf. Sci.* **1992**, *39*, 525.

S0743-7463(96)02021-5 CCC: $14.00

resolution images of molecules such as DNA bases (adenine, guanine, and cytosine) adsorbed on HOPG and Au(111) in electrolyte solutions.[20−23] In another study, xanthine and its oxidized form[24] and porphyrins[25] were found to form ordered adlayers on HOPG. Further, the order−disorder transition in a monolayer of 2,2′-bipyridine on Au(111) was reported as a function of electrode potential.[26] In our recent work, adlayer structures of benzene on well-defined Rh(111) and Pt(111) were determined in HF solutions by using in situ STM.[27] The $c(2\sqrt{3}\times3)$-rect structure was transformed into (3×3)-$1C_6H_6$ and $(\sqrt{21}\times\sqrt{21})R10.9°$ on Rh(111) and Pt(111), respectively.[27]

Although a number of successful experiments using STM and AFM have been performed to determine the structure of organic adlayers on the various substrates described above, the role of interactions between molecules and substrates in ordering processes is not fully understood yet. We discovered a novel substrate with great generality, on which various organic molecules such as porphyrin and crystal violet were found to form highly ordered adlayers.[28,29] The substrate was an iodine monolayer adsorbed on the Au(111) surface, the so-called iodine-modified Au (I-Au). A water-soluble 5,10,15,20-tetrakis-(*N*-methylpyridinium-4-yl)-21*H*,23*H*-porphine (TMPyP) strongly adsorbed on well-defined Au(111) but did not form ordered adlayers, whereas a highly ordered adlayer of TMPyP was visualized on the I-Au(111) electrode by in situ STM with surprisingly high resolution.[28] The formation of ordered TMPyP adlayers was also found to occur on other iodine-modified metal electrodes such as Ag-(111).[30,31] It is striking that such a simple modification of metals surfaces with iodine monolayers allows determination of internal molecular structures, orientations, and packing arrangements of organic molecules with an unusually high resolution achieved in solution. Our recent results[28−31] strongly suggest that the interaction between the molecule and the electrode surface is one of the most important factors determining the formation of ordered adlayers of organic molecules on the substrates in solution.

In this study, we elucidated the effect of the iodine monolayer on the formation of ordered adlayers of TMPyP using both bare and I-Au(111) electrodes in 0.1 M $HClO_4$. Our attention was also focused on the dynamic processes associated with the formation of TMPyP adlayers. Time-sequenced in situ STM images allowed us to reveal several transitional structures developed before the formation of the most thermodynamically stable adlayer.

Experimental Methods

Well-defined bare Au(111) and I-Au(111) electrodes were prepared in the same manner as described previously.[32−34] An Au(111) facet formed on a single-crystal bead was used for STM measurements. For voltammetric measurements, the Au single-crystal bead was cut and mechanically polished with successively finer grades of Al_2O_3. The Au(111) electrode was annealed in a H_2-O_2 flame and quenched in pure water saturated with H_2. To prepare an I-Au(111) electrode surface, the flame-annealed Au electrode was immersed into 1 mM KI solution for 3 min and then rinsed thoroughly with 0.1 M $HClO_4$.[33,34] The electrode was transferred into an electrochemical cell containing 0.1 M $HClO_4$.

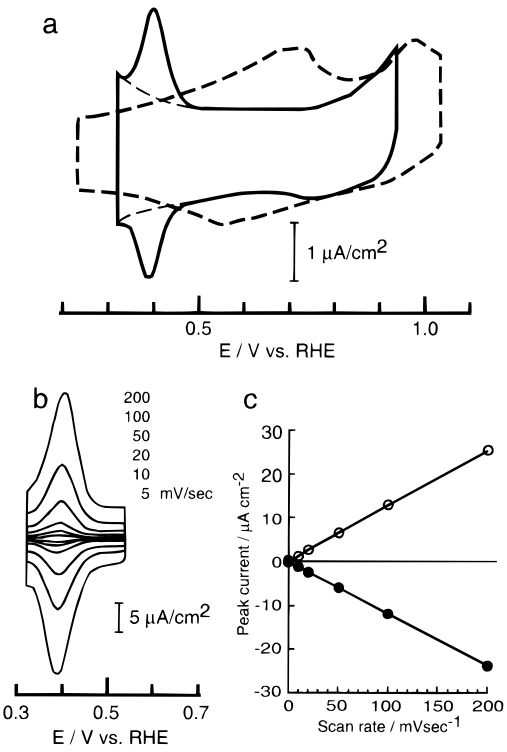

Figure 1. Cyclic voltammograms (a and b) and plots of peak currents *vs* scan rates (c) observed on a bare Au(111) electrode in 0.1M $HClO_4$ in the absence (dotted line) and presence (solid lines) of 5×10^{-7} M TMPyP. The scan rate in (a) was 20 mV/s. The voltammograms in (b) were recorded with scan rates as indicated.

TMPyP (*p*-toluenesulfonate) (Doujin Co. Ltd., Japan) was used without further purification. A dilute aqueous solution of TMPyP, typically $(1-5)\times10^{-7}$ M, was usually injected into 0.1 M $HClO_4$ under potential control in the STM experiments after determination of the structure of the iodine adlayer.

In situ STM measurements were carried out with a Nanoscope III (Digital Instruments, Santa Barbara, CA). The tunneling tip was prepared from an electrochemically etched W wire, and its side wall was sealed with transparent nail polish to minimize the faradaic current. The tip was previously soaked in the electrolyte solution for several hours to remove soluble contaminants before STM measurements were started.[28−30] All images were collected in the constant current mode to evaluate corrugation heights of adsorbed TMPyP molecules. Two Pt wires were used as reference and counter electrodes in the STM cell, respectively. All potentials are quoted with respect to a reversible hydrogen electrode (RHE) in 0.1 M $HClO_4$.

The molecular model for TMPyP was calculated using the MOPAC computer program in the CAChe software package (CAChe Scientific Co. Ltd., USA). The numerical values for TMPyP molecules, such as interatomic distances and size, were estimated from this molecular model.

Results and Discussion

Voltammetry. Figure 1a shows cyclic voltammograms (CV's) of a bare Au(111) electrode in 0.1 M $HClO_4$ in the

(19) Siegenthaler, H. In *Scanning Tunneling Microscopy II*; Wiesendanger, R.; Guntherodt, H. J., Eds.; Springer-Verlang: New York, 1992; Chapter 2, pp 7−49.
(20) Srinivasan, R.; Murphy, J. C.; Fainchtein, R.; Pattabiraman, N. *J. Electroanal. Chem.* **1991**, *312*, 293.
(21) Srinivasan, R.; Gopalan, P. *J. Phys. Chem.* **1993**, *97*, 8770.
(22) Tao, N. J.; DeRose, J. A.; Lindsay, S. M. *J. Phys. Chem.* **1993**, *97*, 910.
(23) Tao, N. J.; Shi, Z. *J. Phys. Chem.* **1994**, *98*, 1464.
(24) Tao, N. J.; Shi, Z. *Surf. Sci.* **1994**, *321*, L149.
(25) Tao, N. J.; Cardenas, G.; Cunha, F.; Shi, Z. *Langmuir* **1995**, *11*, 4445.
(26) Cunha, F.; Tao, N. J. *Phys. Rev. Letts.* **1995**, *75*, 2376.
(27) Yau, S.-L.; Kim, Y.-G.; Itaya, K. *J. Am. Chem. Soc.* **1996**, *118*, 7795.
(28) Kunitake, M.; Batina, N.; Itaya, K. *Langmuir* **1995**, *11*, 2337.
(29) Batina, N.; Kunitake, M.; Itaya, K. *J. Electroanal. Chem. Soc.* **1996**, *405*, 245.
(30) Ogaki, K.; Batina, N.; Kunitake, M.; Itaya, K. *J. Phys. Chem.* **1996**, *100*, 7185.
(31) Batina, N.; Kunitake, M.; Ogaki, K.; Kim, Y.-G.; Wan, L.-J.; Itaya, K., manuscript in preparation.
(32) Yamada, T.; Batina, N.; Itaya, K. *J. Phys. Chem.* **1995**, 99, 8817.
(33) Batina, N.; Yamada, T.; Itaya, K. *Langmuir* **1995**, *11*, 4568.
(34) Sugita, S.; Abe, T.; Itaya, K. *J. Phys. Chem.* **1993**, 97, 8780.

absence (dotted line) and presence (solid line) of TMPyP, respectively. The CV shown by the dotted line was obtained in the double layer potential range between 0.22 and 1.2 V vs RHE. The broad quasi-reversible peaks observed in this potential range are in good agreement with the data reported in the literature.[35,36] In subsequent anodic scans, two well-separated oxidation peaks were found at 1.35 and 1.55 V as described previously,[37] indicating that the surface was a well-defined Au(111) free from contamination.

After the CV of the bare Au(111) was recorded, a TMPyP solution was injected into the electrochemical cell at 0.8 V. The average concentration of TMPyP in the cell was ca. 5×10^{-7} M. The electrode potential was held at 0.8 V for more than 20 min in order to establish an equilibrium state. In this experiment new reversible peaks were found at 0.39 V that had a great stability upon repeated potential cycles. The cathodic and anodic peak currents were almost the same in magnitude and increased linearly with the scan rate as shown in Figure 1, b and c, suggesting that the reversible peaks were due to the redox reaction of the TMPyP molecules adsorbed on Au(111). The half-width of the peaks was found to be 50−60 mV in the range of scan rate between 5 and 200 mV/s. The electrochemical reduction of metal-free TMPyP in acidic solutions was previously investigated.[38,39] The result indicated it to be an overall two-electron process involving the diacid, cation radical, dimethene, and monocation of TMPyP.[38,39] After correction for the background charging current shown in Figure 1a, the total amount of charge consumed for the surface redox reaction was found to be about 8 μC/cm^2 on the average. This value corresponds to a surface concentration of ca. 2.5×10^{13} molecules/cm^2 if the two-electron process is assumed.

Figure 2 shows CV's obtained with an I-Au(111) electrode in 0.1 M $HClO_4$ in the absence (dotted line) and presence (solid line) of 5×10^{-7} M TMPyP. It was shown in our previous papers[33,34] that a featureless voltammogram was observed on an I-Au(111) electrode in pure 0.1 M $HClO_4$, when the potential scan was limited to the double-layer region between 0.4 and 1.1 V. The double layer capacitance decreased substantially on the I-Au(111) compared with that on the bare Au(111), the value for the I-Au(111) being ca. 14−15 μF/cm^2 at potentials around 0.6 V. The cathodic current commencing at 0.3 V in the absence of TMPyP is due to the reductive desorption of iodine adsorbed on Au(111).[33,34] On the other hand, the reversible peaks at ca. 0.3 V for the adsorbed TMPyP were clearly seen on the I-Au(111) electrode in the presence of TMPyP. Although the cathodic and anodic peak currents were also found to increase linearly with scan rate as shown in Figure 2b,c, the half-width of ca. 120 mV observed on I-Au(111) was larger than that on the bare Au shown in Figure 1. It is interesting to note that the peak potentials observed on I-Au(111) were shifted negatively by ca. 100 mV with respect to those found on bare Au(111). These differences in the half-width and the peak potential may have resulted from a flat-lying TMPyP adlayer being formed on I-Au(111). The surface redox reaction of metal-free TMPyP is expected to depend on its orientation on the electrode surface. The surface concentration on I-Au(111) was also evaluated from the total charges consumed during the redox reaction by

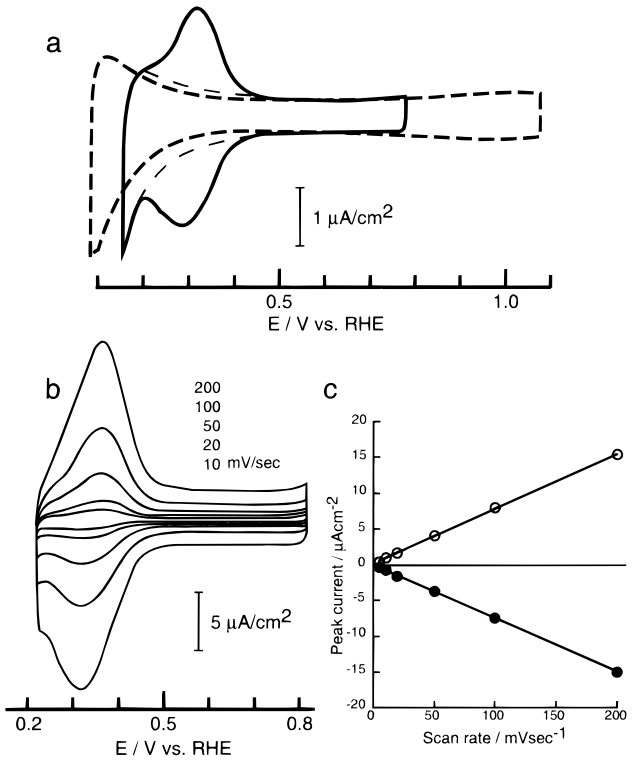

Figure 2. Cyclic voltammograms (a and b) and plots of peak currents *vs* scan rates (c) observed on an iodine-modified Au(111) electrode in 0.1M $HClO_4$ in the absence (dotted line) and presence (solid lines) of 5×10^{-7} M TMPyP. The scan rate in (a) was 20 mV/s.

assuming the two-electron process, yielding values in the range of $(3.1-3.4) \times 10^{13}$ molecules/cm^2. The values obtained on I-Au(111) were significantly larger than those observed on the bare Au(111), suggesting that a more closely packed molecular adlayer is formed on I-Au(111) as discussed later.

We also carried out voltammetric studies in 0.1 M $HClO_4$ containing 1 mM KI. Reversible peaks for the redox reaction of adsorbed TMPyP similar to those shown in Figure 2 were observed. In a 0.1 M $HClO_4$ + 1 mM KI solution containing no TMPyP, characteristic small peaks were found at ca. 0.6 V, which were previously assigned to the phase transition between the centered rectangular $c(p\times\sqrt{3}R\text{-}30°)$ and rotated-hexagonal phases.[32,40] However, these peaks were found to disappear upon adsorption of TMPyP, suggesting that the structure of iodine on Au(111) was also affected by the adsorption of TMPyP on top of the iodine adlayer. Similar reversible peaks with a half-width of 60 mV were found at 0.3 V on HOPG, indicating that TMPyP was also adsorbed on this substrate. Iron and zinc protoporphyrins adsorbed on HOPG have previously been invesitgated by Tao et al. using in situ STM and AFM.[25]

In Situ STM on Bare Au(111). An Au(111) facet formed on the single-crystal bead was first investigated using in situ STM in pure 0.1 M $HClO_4$. Atomically flat wide terrace-step features were consistently found on the Au(111) face in the potential range between 0.7 and 1.1 V, revealing Au(111)-(1×1) atomic images as described previously.[41] Typical widths of the atomically flat terraces were ca. 100−200 nm, indicating that the facet formed on the single-crystal bead is a well-defined Au(111) surface.[37]

(35) Angerstein-Kozlowska, H.; Conway, B. E.; Hamelin, A.; Stoicoviciu, L. *J. Electroanal. Chem.* **1987**, *228*, 429.
(36) Shi, Z.; Lipkowski, J.; Gamboa, M.; Zelenay, P.; Wieckowski, A. *J. Electroanal. Chem.* **1994**, *366*, 317.
(37) Honbo, H.; Sugawara, S.; Itaya, K. *Anal. Chem.* **1990**, *62*, 2424.
(38) Langhus, D. L.; Wilson, G. S. *Anal. Chem.* **1979**, *51*, 1139.
(39) Forshey, P. A.; Kuwana, T. *Inorg. Chem.* **1981**, *20*, 693.
(40) Ocko, B. M.; Watson, G. M.; Wang, J. *J. Phys. Chem.* **1994**, *98*, 897.
(41) Hachiya, T.; Honbo, H.; Itaya, K. *J. Electroanal. Chem.* **1991**, *315*, 275.

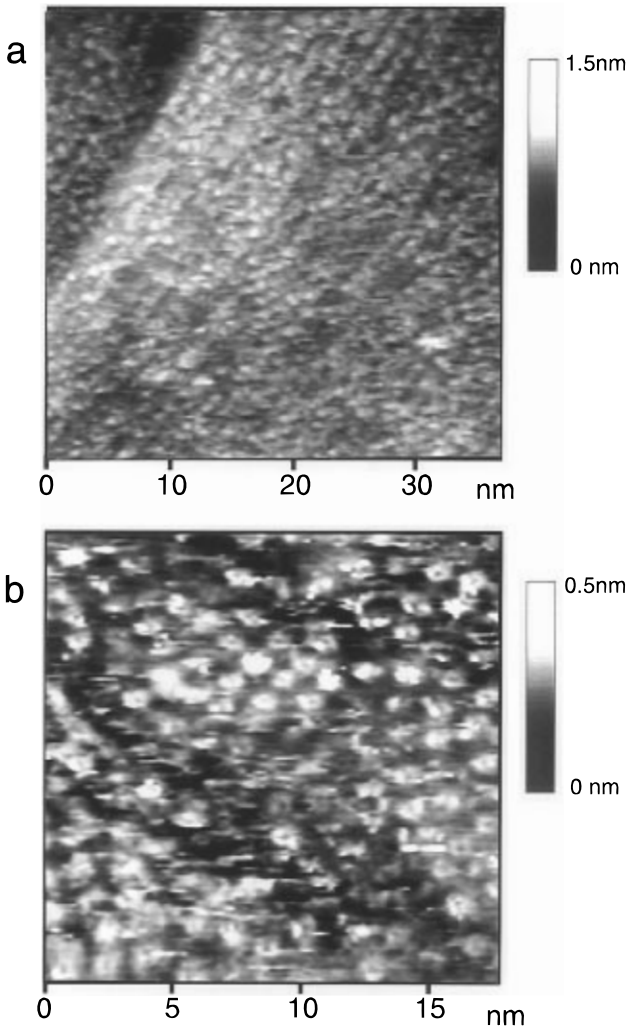

Figure 3. STM images of TMPyP molecules adsorbed on bare Au(111) in 0.1 M $HClO_4$ containing 5×10^{-7} M TMPyP. The images were obtained with a tunneling current (I_t) of 0.35 nA. The electrode potentials of the substrate (E_s) and the tip (E_t) were 0.8 and 0.3 V, respectively.

After the examination of the bare Au surface by STM, a dilute aqueous solution of TMPyP was injected directly into the STM cell under potential control at 0.8 V.

After the injection, bright spots with a diameter of ca. 1 nm immediately appeared on the atomically flat terraces and covered the entire area of the surface. Figure 3a shows a typical large scale STM image of the Au(111) surface acquired after 30 min at 0.8 V. It is clear that both the upper and lower terraces are almost completely covered by these spots, which are presumably due to adsorbed TMPyP molecules. Corrugation amplitudes of these spots were in the range of 0.05−0.1 nm. From the lack of regular patterns in the STM image it can be recognized that the adsorption of TMPyP took place randomly on the bare Au surface. Figure 3b shows one of the highest resolution images acquired on the terrace shown in Figure 3a. Regularities in short range can be found in some areas of the image. For example, several spots are aligned on a straight line with intermolecular distances ranging from 1.7 to 1.9 nm. Shorter distances of ca. 1.3 nm are also seen. Although most spots appeared in rounded or elongated shapes, some spots in the lower-right corner showed the characteristic square shape of TMPyP, which is expected from the structure model of the TMPyP molecule shown in Figure 4. The images shown in Figure 3 directly indicate that TMPyP molecules are adsorbed on Au(111) not only in flat orientation but also in tilted

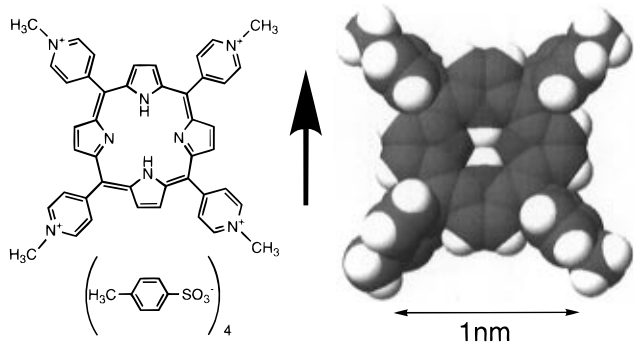

Figure 4. Chemical structure and space-filling model of TMPyP.

or even partially overlapped orientations. We acquired a series of STM images of the same area shown in Figure 3b as a function of time. No changes in either the location of the spots or the appearance of the ordered structure were found over a 1 h period. These results imply that TMPyP molecules are irreversibly adsorbed on Au(111), and the surface mobility of each adsorbed molecule is very low. Similar images were obtained when the electrode potential was changed between 0.6 and 1.0 V, indicating that neither potential dependent phase transition nor improvement in the ordering took place on the bare Au-(111).

In Situ STM on I-Au(111). The experimental procedure described in the preceding section was also applied to the investigation of the adsorption of TMPyP on I-Au-(111). An I-Au single-crystal bead was transferred into the STM cell, and the structure of the iodine adlayer was first examined by in situ STM. The iodine adlayer on Au(111) in 0.1 M $HClO_4$ in the absence of KI was previously investigated by in situ STM and ex situ LEED.[33,34] A centered rectangular $c(p\times\sqrt{3}R\text{-}30°)$ phase was found in the potential range between 0.5 and 1.2 V with a small change in the p value around 2.5.[33] The rotated hexagonal phase appeared at potentials more positive than 1.3 V.[33,34] We confirmed these previous results in this study. Before the injection of TMPyP solution, experimental conditions for achieving high resolution were established by examining the structure of the iodine adlayer. After achieving atomic resolution, a TMPyP solution was injected into the cell. Usually within the first few minutes after addition of TMPyP, no significant changes were observed with only the iodine adlayer structure being resolved. However, the STM image for the iodine adlayer became unclear as time elapsed, and then adsorbed TMPyP molecules became visible in STM images, following the formation of several ordered structures. The dynamic processes will be discussed in the next section.

Eventually, the atomically flat terraces of the I-Au-(111) surface were completely covered by a highly-ordered adlayer of TMPyP after 30 min. Ordered domains usually extended over a large area of the surface as described previously.[28] Figure 5a shows a typical example of high-resolution STM images acquired in a highly-ordered TMPyP domain at 0.8 V. Despite the relatively large area of the image, it is surprising that the orientation of each molecule can be clearly distinguished. TMPyP molecules are perfectly aligned with the same orientation in each row along the direction parallel to the arrow I. Note that a phase boundary can also be seen as indicated by the dashed line. Two domains are simply shifted by a half position. This type of phase boundary was frequently observed along the direction of I as shown previously,[28] whereas boundaries along the directions of II and III were rarely observed.

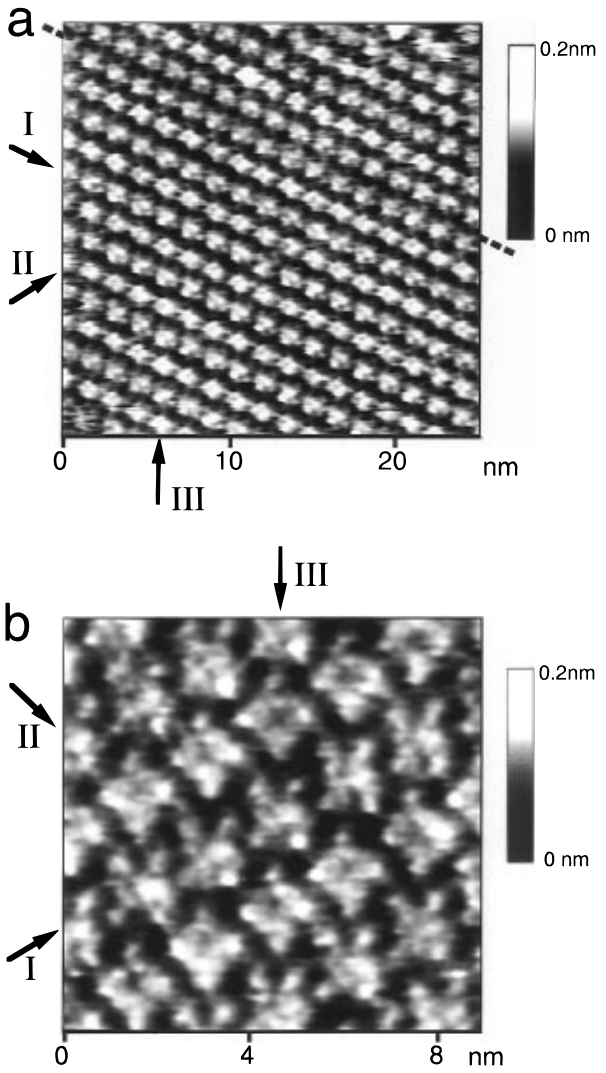

Figure 5. High-resolution STM images of TMPyP adlayers on iodine-modified Au(111) in 0.1 M $HClO_4$ containing 5×10^{-7} M TMPyP. Image (a) was obtained at $E_s = 0.8$ V and $E_t = 0.3$ V; $I_t = 2$ nA. The dashed line indicates a phase boundary. Image (b) was obtained at $E_s = 0.8$ V and $E_t = 0.3$ V; $I_t = 4$ nA.

The image shown in Figure 5b reveals additional details about the symmetry and orientation of the TMPyP molecules in the adlayer. Each flat-lying TMPyP molecule can be recognized regularly in the image as a square shape with characteristic four additional spots (0.4−0.5 nm in diameter) placed at the corners. The shape of the observed features in the image reminds of the real chemical structure and the space-filling model of the TMPyP molecule shown in Figure 4. The high resolution achieved in solution is comparable to or even better than that of similar molecular images of compounds such as Cu phthalocyanine reported in ultra-high vacuum (UHV) conditions.[6] As can be seen in Figure 5a,b, the nearly close-packed molecular array is well-organized two-dimensionally. The molecular rows consist of flat-lying TMPyP molecules with two different rotational orientations on the surface. Two different molecular rows, which are marked by arrows I and II in Figure 5, cross each other at ca. 60°. It is now clear that all TMPyP molecules possess the same orientation in the row marked I. The molecular axis indicated in Figure 4 is rotated by ca. 15° with respect to the direction of I. On the other hand, alternating orientations can be seen in row II, in which every second molecule shows the same orientation. The molecular axes are alternately rotated by 15° or 60° with respect to the direction of II. It is more clearly seen that

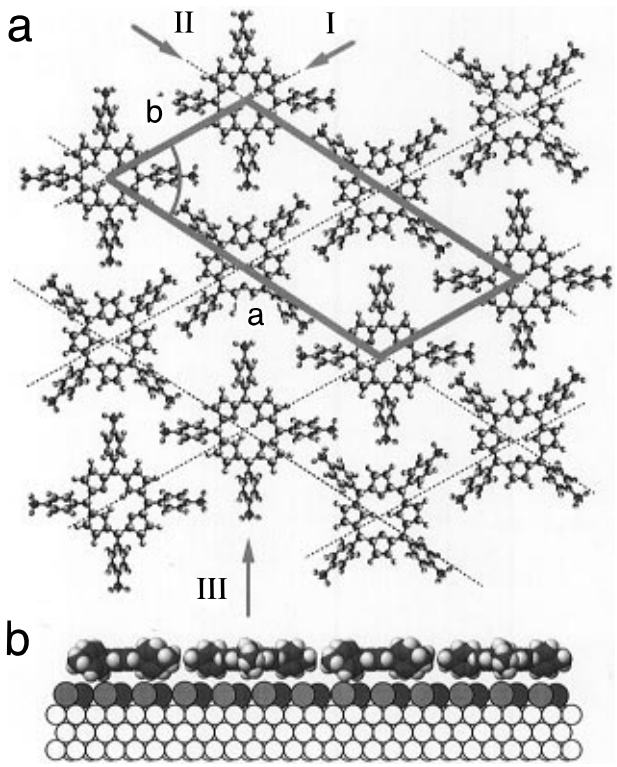

Figure 6. Illustrative depictions of the structure of TMPyP adlayer: (a) top-view, (b) side-view.

the molecular axes in row III are either parallel to or rotated by 45° with respect to the direction of III, in which every second molecule shows the same orientation similarly to row II. These different angles of rotation of the molecules in a given row can result from the fact that repulsive interactions between positively charged pyridinium units are minimized in the thermodynamically stable adlayer. Based on the image shown in Figure 5b, the adlayer structure is illustrated in Figure 6 with an oblique unit cell with lattice parameters of $a = 3.4 \pm 0.2$ nm and $b = 1.8 \pm 0.1$ nm, and with an angle of ca. 60°. A schematic depiction of the side view along the direction of III is shown in Figure 6b, in which the relative sizes of Au and I-atoms and TMPyP molecules are drawn to scale. Each unit cell includes two TMPyP molecules, which corresponds to a surface concentration of ca. 3.7×10^{13} molecules/cm^2. Surface concentration estimated from the STM image is fairly consistent with that obtained by the voltammetric experiment for Figure 2. The smaller value found on the bare Au(111) must be due to the formation of disordered adlayers as shown in Figure 3. These disordered adlayers are expected to have less packing densities on the bare Au(111) surface.

Although we thought that the directions of the TMPyP molecular rows were regulated by the structure of underlying iodine adlayers with specific commensurate relations, the present results obtained on I-Au(111) did not show a clear correspondence between the TMPyP and iodine adlayer structures. In the STM image shown in Figure 5a, the molecular row I was found to be nearly parallel to one of the $\sqrt{3}$ directions of Au(111), while this correspondence was not always observed in our experiments. However, we have recently reported that ordered molecular rows of TMPyP were propagated along the $\sqrt{3}$ direction on an iodine-modified Ag(111) in an alkaline solution.[30] Further work is needed to evaluate the commensurate relation on I-Au(111).

The same structure was consistently observed in the potential range between 0.5 and 1.1 V. No potential-

dependent structural change was observed. At more positive potentials than 1.1 V, the adlayer disappeared because of the oxidation of iodine adlayer as described previously.[33,34] We tried to determine the adlayer structure of the reduced form of TMPyP. However, when the potential reached the region near the onset of the reduction peak shown in Figure 2, STM images such as those shown in Figure 5 gradually became unclear, and only the iodine lattice was occasionally observed at 0.35 V. The iodine adlattice image also gradually disappeared at potentials less positive than 0.3 V because of the reductive desorption of iodine.[33] These results suggest that the reduced form of TMPyP may not form an ordered structure because of the partial desorption of iodine, although the CV's shown in Figure 2b indicate that the reduced form is also strongly attached to the surface of I-Au(111).

The TMPyP adlayer was stable even in pure $HClO_4$ containing no TMPyP. After the acquisition of the images shown in Figure 5, the electrolyte solution containing TMPyP was repeatedly replaced by 0.1 M $HClO_4$. However, an almost identical molecular packing arrangement was observed in the above-mentioned potential range, indicating that TMPyP molecules were irreversibly adsorbed on the iodine adlayer and stayed on the surface with the structure unchanged even in pure $HClO_4$. The adsorption of TMPyP was also investigated in a 0.1 M $HClO_4$ solution containing 1 mM KI at potentials more positive than corresponding to the phase transition peaks described above. Before the injection of the solution of TMPyP, the iodine adlayer was investigated at 0.7 V using STM, which showed a characteristic Moire pattern for a rotated hexagonal phase as reported previously.[32−34] After the confirmation of the rotated-hexagonal structure, a suitable aqueous solution of TMPyP was directly added into the cell at the same potential. The Moire pattern became gradually unclear. After 30 min the adlayer structure was very similar to that illustrated in Figure 6, suggesting no dependence on the initial structure of iodine adlayers. As described previously,[28] imaging with a tunneling current greater than 40 nA can reveal the underlying iodine adlayer without destroying the TMPyP adlayer. It was found that STM images of the iodine structure transparently observed in this manner did not show a Moire pattern. All iodine atoms yielded an equal corrugation amplitude, indicating that the rotated hexagonal phase transformed into a centered rectangular $c(p\times\sqrt{3}R\text{-}30°)$ phase upon adsorption of TMPyP. These STM results seem to be consistent with the result of CV's as described above, where the peaks due to the phase transition disappeared in the solution containing TMPyP. It is clear that the adsorption of TMPyP strongly influences the structure of underlying iodine adlayers.

Dynamic Processes. The in situ STM study also allowed us to evaluate dynamic processes of the formation of ordered TMPyP adlayers on I-Au(111). In order to follow time-dependent processes in the growth of ordered phases, a more dilute solution of TMPyP (ca. 1×10^{-7} M) was employed. Approximately 15 min after adding the TMPyP solution, flat-lying TMPyP molecules began to be observed with its characteristic shape as shown in Figure 7a. The image shown in Figure 7b was acquired at nearly the same location, 20 s after Figure 7a was obtained. Many flat-lying TMPyP molecules can be recognized as squares with four bright spots at the corners of each square. The molecules were aligned one-dimensionally, forming molecular chains at the early stage of the formation of the ordered phase. Adjacent molecules in each chain were aligned with each other with a side-by-side configuration. Two pairs of pyridinium rings in the molecule seemed to be attached to those of the adjacent molecules. From

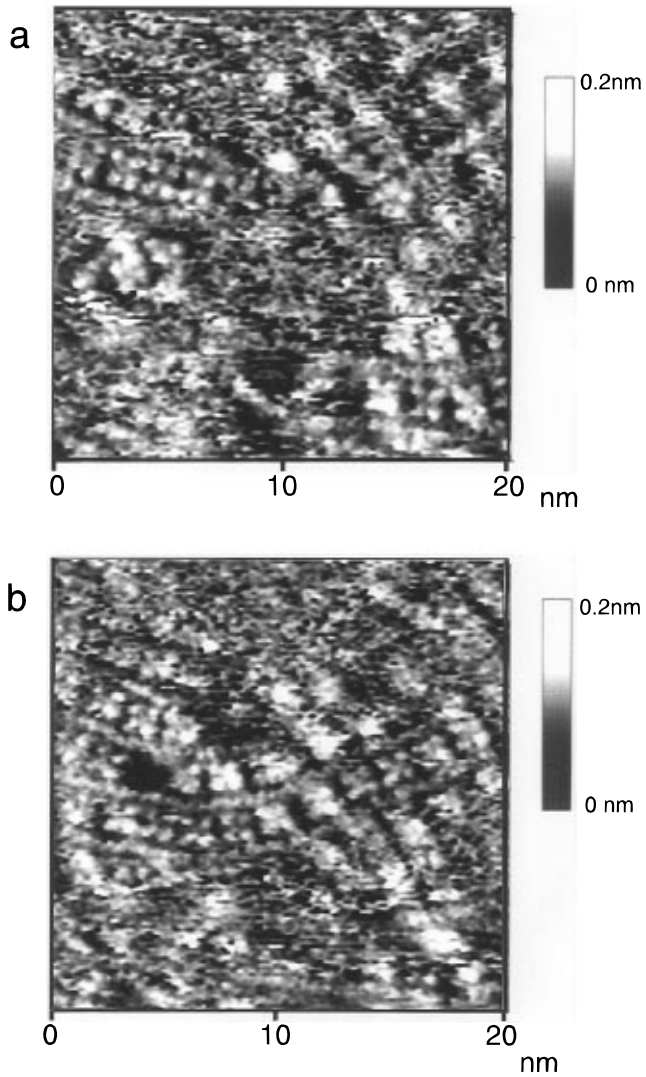

Figure 7. STM images of adsorbed TMPyP molecules at early stages on iodine-modified Au(111) in 0.1 M $HClO_4$ containing 1×10^{-7} M TMPyP. The images were recorded at $E_s = 0.8$ V and $E_t = 0.3$ V; $I_t = 1$ nA. The two images were acquired successively with a time interval of 20 s.

Figure 7, it can be seen that such chains grew relatively rapidly during the time interval of 20 s. The molecular chains are partially straight over a short range, but they form long-twisted lines. During the continuous imaging after the acquisition of the image shown in Figure 7b, it was found that the relative location and shape of the chains in the images always changed rapidly. The intermolecular distance between two adjacent molecules in each chain varied in the range between 1.7 and 2.2 nm. These results strongly indicate that the adsorbed TMPyP molecules have a relatively large surface mobility on the iodine adlayer, which is in contrast to the result found on the bare Au(111) surface as described above. The formation of the molecular chains seems to involve a weak coordination of counter anions, presumably perchlorate, compensating for the repulsive interaction between the positively charged pyridinium units. Isolated molecules usually appeared as simple spots without exhibiting the characteristic shape of TMPyP, which can be seen in the upper right-hand portion of the image in Figure 7a. This result suggests that the isolated molecules undergo not only lateral movements but also rotations in parallel with the surface.

These twisted one-dimensional chains described above were found to become straight and form new two-

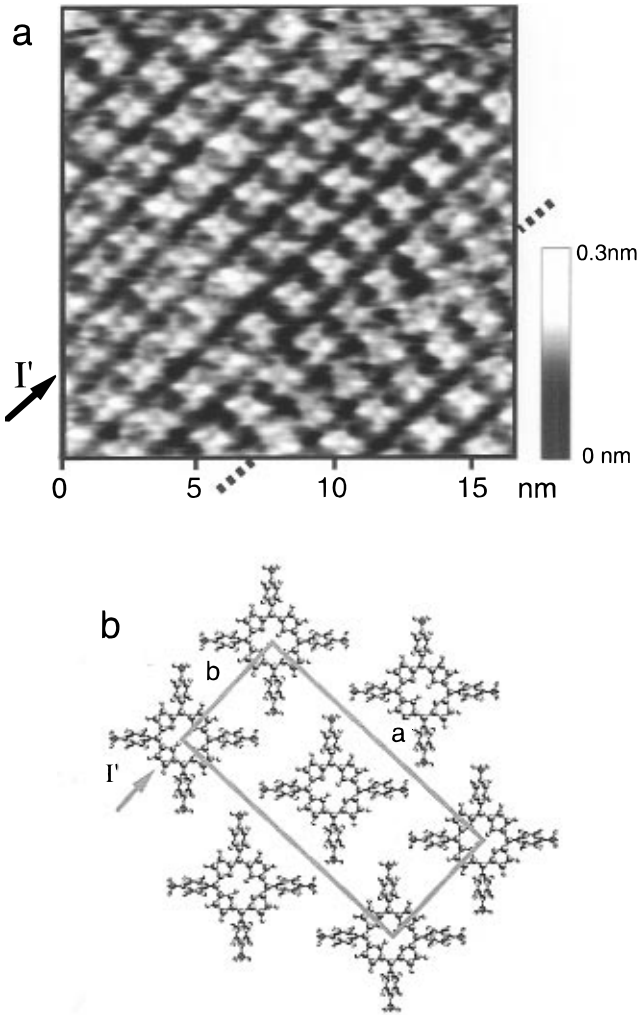

Figure 8. STM image (**a**) and model structure (**b**) of a TMPyP molecular array observed as a transitional phase. The image was recorded at $E_s = 0.8$ V and $E_t = 0.3$ V; $I_t = 4$ nA. The dashed line indicates a row with rotated TMPyP molecules.

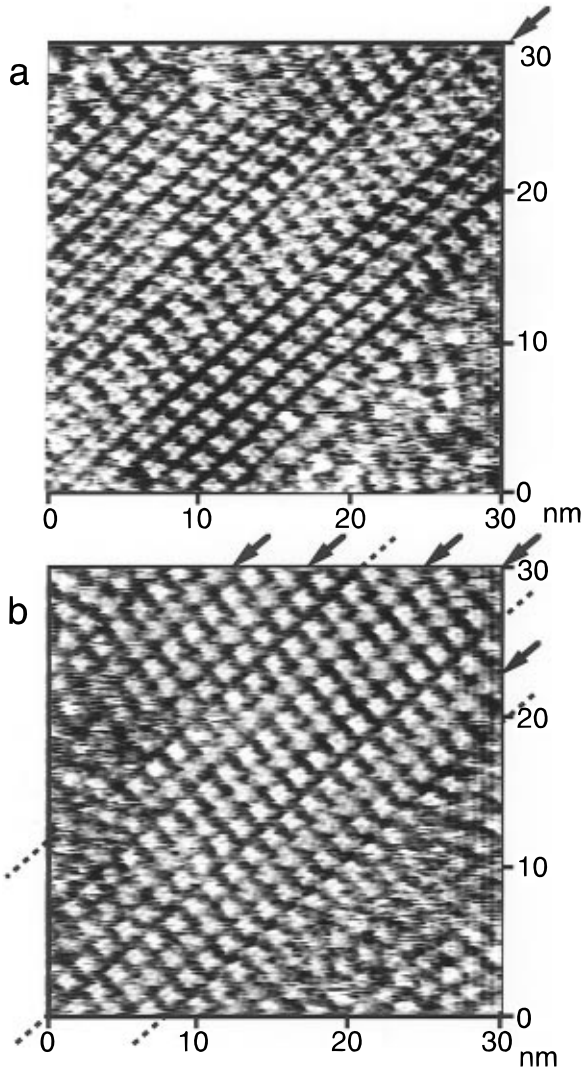

Figure 9. STM images acquired consecutively during phase transition at an early stage of the formation of TMPyP arrays. Each image was obtained in 12 s at $E_s = 0.8$ V and $E_t = 0.3$ V; $I_t = 4$ nA. The arrows indicate the rows with rotated molecules. The dashed lines indicate phase boundaries.

dimensionally ordered arrays in a relatively small domain as a transitional phase. Figure 8a shows an example of images acquired in an initially formed small domain. It is surprising that the molecular chains with the same side-by-side configuration grew in the particular direction indicated by the arrow I′, forming nearly perfect straight lines. The orientation of each molecule in all chains is the same; i.e., the side-by-side configuration and the intermolecular distance in each chain were found to be ca. 1.8 nm. The distance between the nearest neighbor chains was ca.1.8 nm. However, the molecular chains were shifted alternately by a half position of each molecule along the direction I′. This alternation seems to have resulted from the minimization of the repulsive interaction between the pyridinium moieties. A model structure is illustrated in Figure 8b with a rectangular unit cell. A unit cell lattice is outlined with the lattice parameters of $a = 3.7 \pm 0.2$ nm and $b = 1.8 \pm 0.1$ nm. The adlayer structure in Figure 8 corresponds to a surface concentration of about 3.0×10^{13} molecules/cm^2, which is slightly smaller than that found for the final structure. All molecules were already rotated by nearly 45° in the molecular row indicated by the dashed line in Figure 8a.

Figure 9 shows two sequentially acquired images in an expanded area at the same location as for Figure 8a with a time interval of 12 s. In Figure 9a, almost all molecules have side-by-side configuration except for those in the row indicated by the arrow. This structure is identical to that shown in Figure 8a. Note that the lower right-hand portion of the image remained as a disordered phase. It was surprising to find that in such a short period of time, all molecules along the rows marked by the arrows in Figure 9b shifted by a half position and rotated by nearly 45° with respect to the orientation of molecules in the unchanged rows. More interestingly, the final structure shown in Figure 5b appeared soon after the acquisition of the image in Figure 9b. This observation indicates that a further rearrangement takes place in a short period of time to form the final stable structure shown in Figure 5. It was expected that during this period of time the molecules in the unchanged rows in Figure 9b would have rotated and their positions slightly changed. In the final stages, all molecules seem to be cooperatively rotated and translated to form the thermodynamically most stable adlayer structure.

These phase transitions can be illustrated by the model structures shown in Figure 10. The side-by-side configuration shown in Figure 10a corresponds to the structure found in the images in Figures 8 and 9a. As a result of the rotation of the molecules in the row marked by the arrows in Figure 10a, the short-lived temporal structure shown in Figure 10b is formed during the phase transition process. The unit cell parameters seem to be unchanged

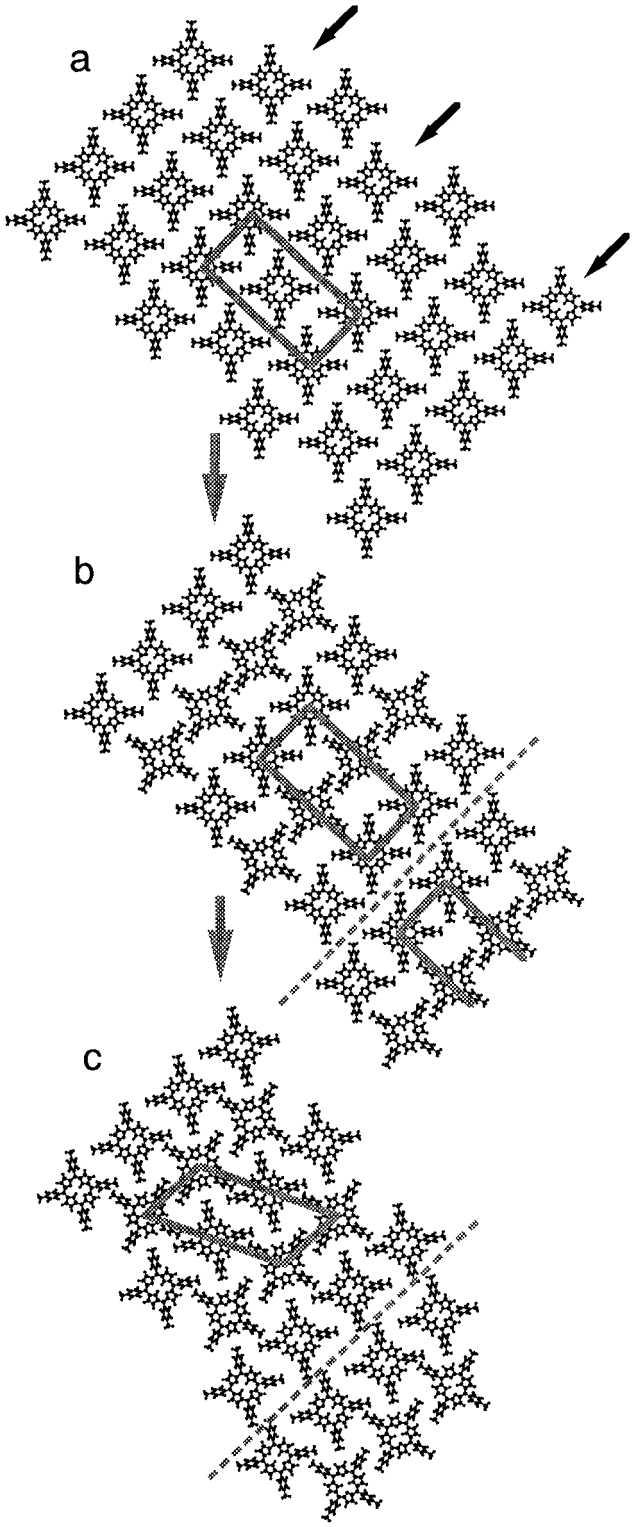

Figure 10. Schematic depiction of phase transition processes observed at early stages (a, b) before the formation of the thermodynamically most stable final structure (c).

during the molecular rotation from Figure 10a to 10b. The molecular rotation in the rows marked by arrows in Figure 10a should occur cooperatively in the same direction either clockwise or counterclockwise, because of the hindrance of rotation brought about by the adjacent pyridinium units as shown in Figure 10b. In the final step to form the structure shown in Figure 10c, the molecules in the rows that remain unchanged in the transition from Figure 10a to 10b are expected to be slightly rotated and translated to establish the most stable structure. Note that the surface concentration of the side-

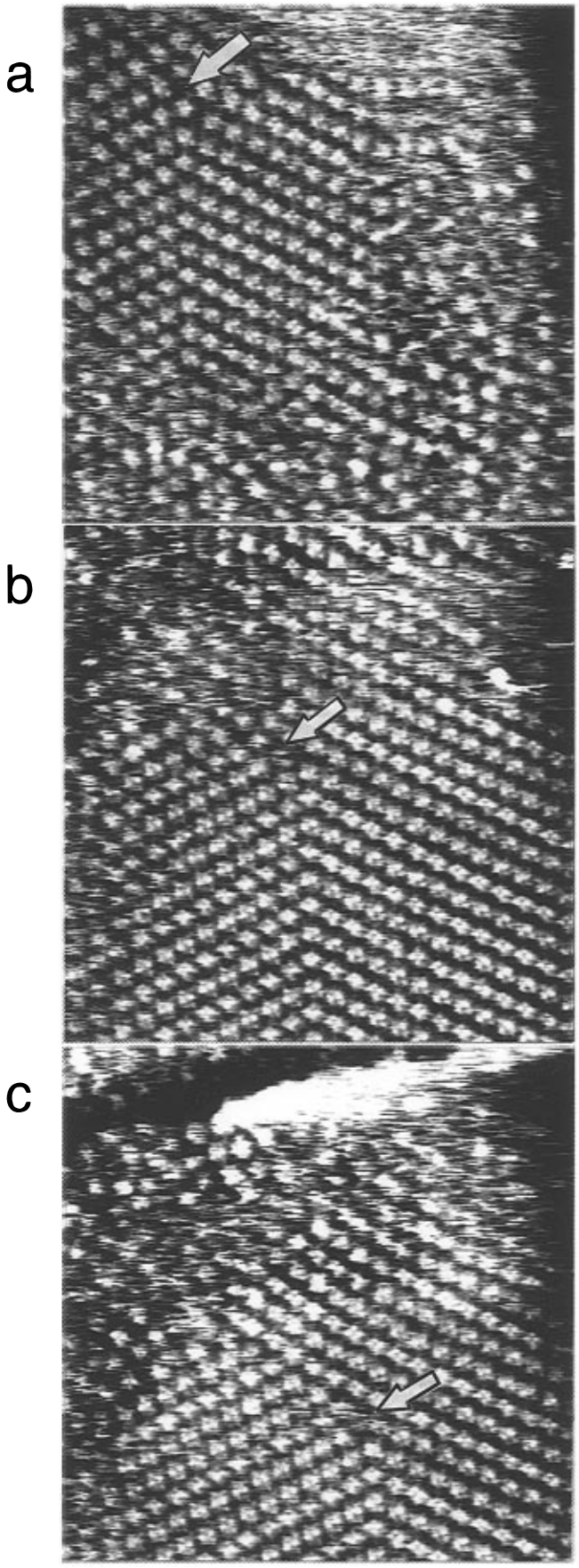

Figure 11. STM images acquired at an early stage of the growth of the most stable TMPyP domain in 0.1M $HClO_4$ containing 5×10^{-7}M TMPyP. The images were recorded at $E_s = 0.8$ V and $E_t = 0.3$ V; $I_t = 4$ nA. Image (b) obtained 4 min after recording (a), and image (c) 6 min after recording (a). The arrows indicate single molecular defects.

by-side structure is ca. 20% smaller than that for the final structure as described above.

The phase boundary more often observed along the direction of I in Figure 5a can be explained by the structural models illustrated in Figure 10. Such a phase boundary is not expected to appear when the molecular rotation occurs only in every second row. As can be seen in Figure 9b, however, the rotation occurred not only in every second row but also in the third row. The dashed lines in Figure 9b indicate the phase boundaries produced by the rotation in the third row. The rotational tranformation occurring in odd-numbered rows is thought to be responsible for the formation of the boundary, which is also illustrated by the dashed lines as in Figure 10, b and c.

The structural transformation in the TMPyP array described above was always found to occur when the domain size of the first stage (Figure 10a) was smaller than several tens of nanometers. Interestingly, once the most stable structure appeared in a domain, it expanded over the entire area of atomically flat terraces with the final packing arrangement. Figure 11 shows a set of STM images acquired in an area where domain boundaries could be seen between the ordered and disordered phases. The images shown in Figure 11, b and c, were obtained with time intervals of 4 and 6 min, respectively, after the image of Figure 11a was acquired. The arrows in the images indicate a single molecular defect located at the cross point of two phase boundaries formed by the rotational domain, which was used as a marker for acquisition of the images. Careful inspection of the image shown in Figure 11a revealed that the ordered domain was already constituted with the final structure illustrated in Figure 10c. The results shown in Figure 11 directly demonstrate that molecules in the disordered phase are progressively incorporated into the ordered domain with the final internal structure. This two-dimensional growth can explain the formation of the highly-ordered TMPyP adlayer extending over the wide area. The ordered domain of the TMPyP adlayer increased in area and expanded in the particular direction along row I. The growth rate along row **I** was substantially greater than the rates along other directions. Using the single molecular defects marked by the arrows in Figure 11 as land-markers, an averaged growth rate of 20 molecules/min was found along row I. We also estimated the growth rate along row II to be very small, ca. 2−3 molecules/min. The results shown in Figure 11 suggest that the intermolecular interaction between adjacent molecules along row I is stronger than that along other directions. A similar anisotropic growth of ordered domains was previously found for TMPyP adsorbed on an iodine-modified Ag(111) electrode.[30]

The phase transition observed in Figure 9 and illustrated in Figure 10 can only be expected to occur when the domain size is less than several tens of nanometers, because the phase transition requires cooperative rotational and translational motions in each ordered phase. The complicated force relationship in the molecular arrays consists mainly of two different interactions: perpendicular interactions between the electrode surface and molecules as a driving force for initial adsorption, and intermolecular interactions for self-organization leading to the formation of the ordered layer. Surface diffusion of adsorbed molecules seems to be a key factor for the ordering process in general. On bare Au(111), TMPyP molecules can not diffuse because of a strong interaction between TMPyP and the Au surface. On the other hand, the relatively weak van der Waals type interaction between the TMPyP molecules and the iodine adlayer on the metal substrate allows the adsorbed molecules to diffuse on the iodine adlayer, resulting in the formation of an ordered molecular phase.

In the expected intermolecular interactions, electrostatic interactions between the positively charged pyridinum units might play a significant role in the determination of the adlayer structure. These positive charges should be balanced by the coordination of anions such as perchlorate in solution. Although high-resolution STM images such as the one shown in Figure 5b did not show additional corrugations due to perchlorate, perchlorate anions are expected to be located near or between the pyridinium rings. Detailed investigations using different anions are of special interest. It is worthwhile to note that TMPyP formed an ordered structure on an iodine-modified Ag(111) in an alkaline electrolyte solution containing KI (0.1 mM KI + 10 mM KF + 0.1 mM KOH at pH 10).[30] In this case, I^-, F^-, and OH^- are expected to contribute to the charge neutrality at the TMPyP adlayer−electrolyte interface.

Finally, TMPyP adsorbed on HOPG was also briefly investigated in the present study in 0.1 M HClO4 + 5×10^{-7} M TMPyP. Unfortunately, no clear molecular images such as those found on I-Au(111) were obtained because of relatively large corrugation amplitudes for the individual carbon atoms of HOPG, which interfered with the observation of the shape of TMPyP molecules. The poor resolution achieved previously for metal protoporphyrins on HOPG might be due to the fact mentioned above.[25] The results shown in this paper clearly demonstrate that the iodine-modified metal electrodes, particularly I-Au single-crystal electrodes, serve as ideal substrates for in situ STM imaging of organic molecules in solution.

Conclusions

A highly-ordered TMPyP array was formed at the iodine-modified Au(111) electrode−electrolyte ($HClO_4$) interface, and its structure was determined by in situ STM, whereas disordered adlayers of TMPyP were found to form on bare Au(111) surface. Iodine adlayer on Au(111) plays a crucial role in the formation of the highly-ordered adlayer. No structural change in the adlayer was found in the double layer potential range, but the ordered adlayer could not be seen at potentials where the iodine adlayer was electrochemically oxidized or reduced. The ordered adlayer also became disordered upon the reduction of TMPyP moiety. In situ STM was successfully applied to observe the dynamics of self-organization processes. The randomly adsorbed TMPyP molecules were aligned one-dimensionally, forming molecular chains at an early stage. Several ordered phases appeared before the final, thermodynamically stable structure of the array was established. The ordered adlayer with side-by-side configuration appeared as a metastable phase. In a relatively short period of time, all molecules in particular rows were cooperatively rotated, and then the final phase appeared as a small domain. Such a small domain grew as a result of incorporation of the adsorbed TMPyP molecules in the disordered phase. This growth mechanism can explain the formation of the highly-ordered adlayer extending over the entire area of the atomically flat terrace.

Acknowledgment. We thank Dr. Y. Okinaka for his helpful discussion in connection with the writing of this manuscript. This work was supported by ERATO-Itaya Electrochemistry Project, JRDC.

LA9620216